

Interannual variation in soil CO₂ efflux and the response of root respiration to climate and canopy gas exchange in mature ponderosa pine

J. IRVINE*, B. E. LAW*, J. G. MARTIN* and D. VICKERS†

*College of Forestry, Oregon State University, Corvallis, OR 97331-5752, USA, †College of Oceanic and Atmospheric Sciences, Oregon State University, Corvallis, OR 97331-5503, USA

Abstract

We examined a 6-year record of automated chamber-based soil CO₂ efflux (F_s) and the underlying processes in relation to climate and canopy gas exchange at an AmeriFlux site in a seasonally drought-stressed pine forest. Interannual variability of F_s was large (CV = 17%) with a range of 427 g C m⁻² yr⁻¹ around a mean annual F_s of 811 g C m⁻² yr⁻¹. On average, 76% of the variation of daily mean F_s could be quantified using an empirical model with year-specific basal respiration rate that was a linear function of tree basal area increment (BAI) and modulated by a common response to soil temperature and moisture. Interannual variability in F_s could be attributed almost equally to interannual variability in BAI (a proxy for above-ground productivity) and interannual variability in soil climate. Seasonal total F_s was twice as sensitive to soil moisture variability during the summer months compared with temperature variability during the same period and almost insensitive to the natural range of interannual variability in spring temperatures. A strong seasonality in both root respiration (R_r) and heterotrophic respiration (R_h) was observed with the fraction attributed to R_r steadily increasing from 18% in mid-March to 50% in early June through early July before dropping rapidly to 10% of F_s by mid-August. The seasonal pattern in R_r (10-day averages) was strongly linearly correlated with tree transpiration ($r^2 = 0.90$, $P < 0.01$) as measured using sap flux techniques and gross ecosystem productivity (GEP, $r^2 = 0.83$, $P < 0.01$) measured by the eddy-covariance approach. R_r increased by 0.43 g C m⁻² day⁻¹ for every 1 g C m⁻² day⁻¹ increase in GEP. The strong linear correlation of R_r to seasonal changes in GEP and transpiration combined with longer-term interannual variability in the base rate of F_s , as a linear function of BAI ($r^2 = 0.64$, $P = 0.06$), provides compelling justification for including canopy processes in future models of F_s .

Keywords: gross primary production, modeling, *Pinus ponderosa*, rhizosphere respiration, root exclusion, soil respiration, transpiration

Received 21 January 2008 and accepted 25 March 2008

Introduction

The ability of forested ecosystems to store carbon is dependent on the balance between photosynthesis and the release of carbon through respiratory processes. The majority of the respiratory release is from the soil (Law *et al.*, 1999; Janssens *et al.*, 2001), and consequently soil CO₂ efflux (F_s) might play a pivotal role in determining the degree to which forested ecosystems are able to store carbon and influence the current rate of change of

atmospheric CO₂. Measuring F_s is relatively easy and much has been learned from determining the magnitude of F_s over various spatial scales covering a range of ecosystems (Raich *et al.*, 2002; Reichstein *et al.*, 2003; Hibbard *et al.*, 2005). However, our quantitative knowledge of the underlying processes that ultimately result in the release of CO₂ from the soil is relatively weak. F_s is often referred to as soil respiration and the use of this term has perhaps obscured the fact that F_s is a result of many underlying processes; principally, F_s is a product of both autotrophic respiration (R_r) and heterotrophic respiration (R_h), and the subsequent transport of CO₂ through the soil profile. Consequently, although

Correspondence: James Irvine, tel. +1 541 737 8456, e-mail: james.irvine@oregonstate.edu

relationships of F_s to environmental variables are often described with mechanistic undertones, such relationships are strictly empirical, site-specific and have limited value beyond the study in which they were derived. Recently, there has been increased activity in partitioning F_s into the underlying components as described in several synthesis papers (Hanson *et al.*, 2000; Kuzyakov, 2006; Subke *et al.*, 2006). In addition, a growing number of publications strongly emphasize the physiological continuity between above- and below-ground processes (Irvine *et al.*, 2005; Hogberg & Read, 2006; Sampson *et al.*, 2007; Stoy *et al.*, 2007), which has been long understood theoretically, but more difficult to quantify (Ryan & Law, 2005). The explicit link between carbon fixation and F_s is poorly defined, and most biogeochemistry models simulate carbon movement from above- to below-ground pools and its subsequent release using a mass balance approach (Luo & Zhou, 2007) that is unsuitable for modeling short-term variation in F_s . With these issues in mind, we have two main objectives in this current study: (1) identify patterns in a multiyear record of F_s and ecosystem processes at an AmeriFlux site to generate a parsimonious seasonal model for F_s that has traits of value to the wider research community, and (2) assess the relationship between substrate supply from the canopy and root/rhizosphere respiration.

Materials and methods

Study site

The site is a semiarid 90-year-old ponderosa pine forest located on the east side of the Cascades Mountains, near Sisters, OR, USA (44.452N, 121.557W), at an elevation of 1255 m. It is one of the Metolius cluster of eddy-covariance sites in different age forests and part of the AmeriFlux network of flux sites. The tree canopy is

almost exclusively ponderosa pine (*Pinus ponderosa* Dougl. ex P. Laws.) with a few scattered incense cedar [*Calocedrus decurrens* (Torr.) Florin] with a leaf area index (LAI) of 2.8. Tree height is approximately 15 m with 325 trees ha⁻¹ and total basal area 24.4 m² ha⁻¹ in 2001, increasing to 31.6 m² ha⁻¹ by 2006. The understory is sparse (LAI = 0.2) comprised largely of bitterbrush [*Purshia tridentata* (Push) D.C.] and Manzanita (*Arctostaphylos patula* Greene). Soils are sandy (67% sand, 7% clay measured over 50 cm depth), freely draining with a soil depth of up to approximately 1.5 m. The area has cool wet winters and hot dry summers with between 300 and 600 mm of precipitation per year, the majority falling between November and April as a combination of rain and snow.

Soil CO₂ efflux and root exclusion

An automated soil chamber system based on the design of Goulden & Crill (1997) was deployed with six chambers in March 2001; specific details of the system used during this study follow methods described in Irvine & Law (2002). The system ran approximately from April through October each year; it was unsuited to operate during the freezing/snowy conditions of winter. Each chamber was measured every 90 min, chambers were left in place (in the open position) throughout the study. During the first 2 years of operation, measurements were made every other 2-week period. During the last 4 years, continuous data were recorded. Over the 6-year period, on average 150 days of useable data per year were logged (Table 1). Soil volumetric moisture content (VMC) integrated over the top 30 cm depth of soil as well as at 10 cm depth (CS615, Campbell Scientific, Logan, UT, USA) was measured together with soil temperature profiles (2, 8 and 16 cm depths) next to each chamber. Daily mean values of F_s and soil climate were used for examining seasonal and

Table 1 Summary of measured and modeled F_s with associated ancillary biological data

| Year | Automated F_s (start/end day) | No. of days | Annual F_s (g C m ⁻² yr ⁻¹) [r^2] | Multiyear r^2 | Annual BAI (m ² ha ⁻¹ yr ⁻¹) | Annual litterfall (g m ⁻² yr ⁻¹) | R_b (g C m ⁻² yr ⁻¹) |
|------|------------------------------------|-------------|-------------------------------------------------------------------|-----------------|-------------------------------------------------------------------|---------------------------------------------------------------|--------------------------------------------------|
| 2001 | 88/292 | 111 | 612 [0.82] | 0.78 | 1.22 | 121.2 | 0.922 |
| 2002 | 95/279 | 110 | 768 [0.75] | 0.57 | 1.27 | 120.6 | 1.002 |
| 2003 | 87/282 | 172 | 806 [0.86] | 0.83 | 1.31 | 270.1 | 1.029 |
| 2004 | 93/286 | 176 | 1039 [0.79] | 0.73 | 1.62 | 170.1 | 1.055 |
| 2005 | 69/298 | 162 | 836 [0.94] | 0.83 | 1.63 | 227.6 | 1.257 |
| 2006 | 110/310 | 174 | 803 [0.91] | 0.83 | 1.39 | 202.4 | 1.007 |
| Mean | 90/291 | 150 | 811 [0.85] | 0.76 | 1.40 | 185.3 | 1.045 |

Annual soil CO₂ efflux (F_s) was estimated using Eqn (1) fitted by year (e.g. Fig. 3). Multiyear r^2 is from the simplified parameterization of Eqn (1) fitted across all years of data in which only the annual base rate (R_b) was allowed to vary linearly with annual tree basal area increment (BAI).

interannual patterns. In spring 2004, four additional automated chambers were added for the root exclusion treatment and the measurement interval increased to 120 min. F_s measurements from the new chambers began 3 months before root exclusion by trenching in late July 2004. A trench approximately 0.25 m wide and 0.6 m deep was dug around each chamber at least 0.5 m from the chamber. All roots were severed and the side walls of the trenches were lined with heavy landscape fabric before being refilled with soil. Soil cores taken to 1 m depth before trenching suggested over 90% of the fine root mass was within 0.5 m of the soil surface. Data from these cores were used to estimate the biomass of freshly severed roots under the trenched soil chambers. Fine root decomposition rates from buried mesh bags at local sites (Law *et al.*, 2001) together with decomposition estimates for larger roots (Chen *et al.*, 2001) were used to correct for the artificial increase in heterotrophic CO_2 efflux in the trenched plots.

To account for spatial variability of F_s across the site that may not be represented by the mean F_s from the automated chambers, manual measurements of soil efflux were made using a Li-6400 with Li-6000-9 soil chamber (LI-COR Inc., Lincoln, NE, USA). On 16 occasions, between spring and fall, manual measurements were made at 18 locations; six polyvinyl chloride collars (10.7 cm diameter, 10.0 cm high) were installed 5 m apart on each of three 30 m transects, these collars were moved to new locations following each set of 18 measurements in order to minimize spatial bias. The collars were installed approximately 2.5 cm into the soil layer so as to avoid severing roots; the remaining height of the collar was largely occupied by the litter layer.

Transpiration

Sap flux was measured each year between April and November using the heat dissipation technique. Twelve trees covering the range of tree diameters on the site were instrumented with a combination of sap flux sensors in the outer sapwood and sensors to measure the radial sap velocity profile with sapwood depth. Data from these probes were used together with surveys of tree diameters on site to compute daily total tree transpiration. More specific methods are given in Irvine *et al.* (2004).

Basal area increment (BAI)

Girth bands constructed from aluminum strapping and small extension springs were installed at 1.3 m height [diameter at chest height (DBH)] in early spring 2001 on 15 trees. These were measured using digital calipers every fall after seasonal radial increment was complete (typically in October). In summer 2002, an additional 69

trees were installed with girth bands and initial measurements made the following year; both sets of trees were measured through 2003 after which only the second group of trees was measured to the current time. The data were used to generate a complete 6-year record of annual basal increment for those trees between 25 and 40 cm DBH (70% of the trees on site), minimizing any bias from a few small trees (average DBH 12 cm) that had large relative basal increment, but contributed insubstantially to absolute changes in site annual basal increment.

Gross ecosystem productivity (GEP)

Eddy-covariance measurements were made using a Campbell Scientific CSAT3 sonic anemometer and open-path LICOR-7500 gas analyzer at 31 m above the ground. Further details of the technique, theory and instrumentation as applied to the Metolius cluster of AmeriFlux sites have been described in Anthoni *et al.* (2002). At this site, missing observations of CO_2 flux and CO_2 storage below the sensor height were gap-filled using the average value based on a composite diurnal cycle for a local 5-day period. The length of this composite cycle was expanded in increments of 5 days for longer gaps. This approach was found to be the most stable method by Falge *et al.* (2001). The eddy-covariance technique directly measures the net ecosystem exchange (NEE) of carbon and an estimation of ecosystem respiration (R_{eco}) was required to determine GEP. For this paper, R_{eco} was computed independently of the automated F_s data using the common approach of describing the temperature sensitivity of night-time NEE (i.e. R_{eco}) under well-mixed conditions and then using this relationship to replace nocturnal estimates of R_{eco} during weak-mixed conditions ($u^* < 0.6$), and to extrapolate R_{eco} into daytime conditions. To select suitable night-time data for the analysis at this site with its weak nocturnal wind speeds, where stable stratification induced by surface radiative cooling strongly suppresses nocturnal turbulence, a critical u^* threshold of 0.6 m s^{-1} was employed (e.g. Goulden *et al.*, 1996; Gu *et al.*, 2005). This was based on the u^* dependence of the nocturnal CO_2 flux and CO_2 storage below the sensor height after removing the temperature and soil moisture dependence, and applying the 95% threshold criteria (Reichstein *et al.*, 2005).

Modeling F_s

To account for the interactive response of F_s to soil temperature and moisture, we use a nonlinear function to describe how these variables modulate the underlying or basal rate of F_s [Eqn (1)]; this function has

previously been shown to adequately describe the response of F_s in ponderosa pine (Irvine & Law, 2002).

$$F_s = R_b \times \exp(k_1 \times T_{16\text{cm}}) \times (1 - (k_2 \times \exp(k_3 \times \delta\theta_{10\text{cm}}))), \quad (1)$$

where R_b is the base rate of F_s modulated by both soil temperature as measured at 16 cm depth ($T_{16\text{cm}}$) and soil water deficit at 10 cm depth ($\delta\theta_{10\text{cm}}$), where δ is expressed relatively between 0 and 1 (minimum and maximum water deficit, respectively) using $\delta = (\theta_{\text{max}} - \theta) / (\theta_{\text{max}} - \theta_{\text{min}})$ where the subscripts max and min refer to the maximum and minimum values of soil water content at 10 cm depth across the 6-year period. k_1 , k_2 and k_3 are fitted parameters. This function is a simple representation of the effects of temperature and moisture on F_s ; in reality, soil contains a diverse range of materials available for decomposition in addition to sources of R_r . Theory suggests an Arrhenius relationship in which the temperature sensitivity of F_s declines with increasing temperature is a more theoretically robust representation of the effect of temperature on decomposition (Davidson & Janssens, 2006). However, a constant temperature sensitivity of F_s is common in the literature, and for simplicity, we chose van't Hoff exponential representation. This representation is consistent with a fixed Q_{10} , defined as the relative increase in F_s for a 10°C increase in temperature and is equal to $e^{k_1 \times 10}$.

This function has four parameters which could be optimized to fit the data, or one or more parameters could be fixed depending on the objectives, prior information and degree of correlation between the parameters. We used this function in two ways to achieve different objectives. To provide the best annual estimate of F_s from seasonal measurements, we fit the function to individual year datasets allowing all four parameters to be optimized (PROC NLIN, SAS 9.1, SAS Institute, Cary, NC, USA), the year-specific parameters were then used to estimate annual F_s for that specific year from continuous soil climate data (Table 1). The parameter estimates generated in this manner cannot be interpreted further and have no value beyond generating a year-specific estimate of F_s , such annual estimates are useful to those in the carbon flux research community. The use of Eqn (1) in this fashion is an improvement over simple interpolation in that it allows a degree of extrapolation based on year-specific measured soil climatic conditions. By generating annual F_s on this basis, we do not lose information about interannual variability in F_s that may be poorly represented by the simple empirical relationship if fitted to a multiyear dataset. The second use of this function was to determine if in fact it could adequately capture interannual variability in F_s when fitted to a multiyear dataset and, if so, what simplifications could be made. Specifically,

we wished to assess if constants could be used in place of parameters and still allow robust annual estimates of F_s to be generated. We seek the most parsimonious use of Eqn (1) and by simplification hoped to gain further insight into F_s . The first simplification involved constraining the soil moisture multiplier to a value between one and zero by fixing k_2 to 0.001. This dictated that the soil moisture multiplier took a value of essentially 1 under no soil water limitations, but as the soil dried, the multiplier fell towards zero at a rate dependent on k_3 thereby reducing F_s . This simplification was applied to all subsequent use of Eqn (1) in this paper.

Functions such as Eqn (1) do not readily allow for dynamic changes in the pool of respiring material unless parameter R_b is allowed to vary with time. Whether other parameters such as the temperature sensitivity (k_1) of F_s should vary with time remains a topic of current debate (Curiel Yuste *et al.*, 2004; Sampson *et al.*, 2007). If several parameters vary through time, it is possible that several combinations of parameters will produce equally good fits to the data but provide no basis for attributing temporal patterns in F_s to a particular mechanism [see Davidson *et al.* (2005) for a well-considered synthesis of this issue]. On the basis of a weak correlation ($r < 0.2$) between R_b and k_1 , and no information to suggest the temperature and soil water sensitivities (i.e. k_1 and k_3) change across the 6-year period, we made a pragmatic decision of assuming a constant temperature and soil water sensitivity but allowed R_b to be optimized each year. The value used for k_1 (0.1, i.e. $Q_{10} = 2.7$) was generated by fitting Eqn (1) to the 6-year dataset and allowing all parameters to be optimized. The value for k_3 (6.563) was generated when k_1 was fixed to 0.1 and only R_b and k_3 allowed to be optimized.

Results and discussion

Estimating site level F_s

The comparison between periodic manual and automated F_s indicated a strong linear relationship ($r^2 = 0.85$, $P < 0.01$) between approaches but with an offset most likely attributed to a spatial bias [i.e. the fixed location of the automated chambers not representing the site spatial mean F_s over several hectares (Fig. 1)]. The slope of the relationship was 0.91 with a 95% CI between 0.66 and 1.14, and therefore, not significantly different from 1. A more detailed analysis also indicated that when soil moisture measured in the top 10 cm layer of the soil exceeded 20% VMC, a larger discrepancy between the two approaches was apparent. This discrepancy may be related to litter quantity and related decomposition with increased soil moisture, as we have not observed this issue on sites with negligible

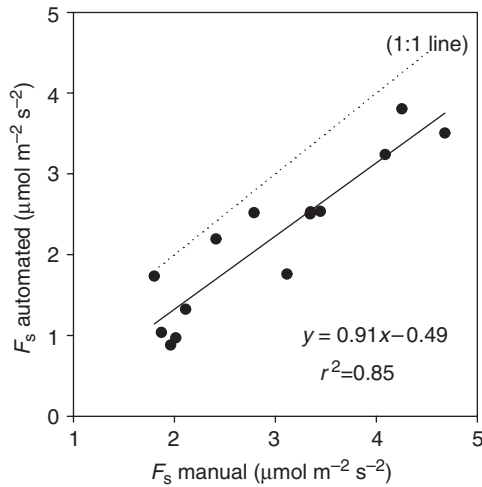


Fig. 1 Comparison of manual and automated soil CO₂ efflux measurements. Each point is the mean of six spatially fixed automated chamber measurements (0.21 m² sampling area per chamber) and 18 manual measurements (0.01 m² sampling area per chamber) that were relocated between each set of measurements at points throughout the study site. The offset from the 1:1 relationship suggests the automated chambers do not directly provide an estimate of the site mean F_s .

litter layer. To account for both the spatial bias and discrepancy between approaches under high-surface soil moisture conditions, we use the ratio of the mean manual F_s (spatially representative) to mean automated F_s (spatially biased) expressed as a second-order polynomial function of soil water content to correct the automated chamber F_s data ($n = 16$, $r^2 = 0.78$). This can be interpreted as the automated chambers underestimating site level F_s by 22% due to spatial bias, and on average, across a season of measurements, the automated chambers would underestimate manual-based F_s by an additional 10% due to discrepancies between approaches under high-moisture conditions. We apply corrections to daily mean-automated F_s on this basis to compute site level daily mean F_s .

Interannual and seasonal patterns of F_s

Interannual and seasonal patterns of measured F_s , soil climate, tree transpiration and tree BAI across the 6-year period expressed as anomalies from the 6-year mean (in units of standard deviation of the mean) are shown in Fig. 2 on a monthly basis (black bars) as well as on an annual basis (gray bars). Using Eqn (1) to estimate annual F_s from each of the annual dataset (see 'Materials and methods'), annual F_s ranged from 612 to 1039 g C m⁻² yr⁻¹ (Table 1; 6-year CV = 17%; 40% difference between minimum and maximum). Concerns that extrapolation of the F_s model during the winter period (November through March, when the automated

chamber could not function) may result in a significant source of interannual variability in F_s were unfounded. Modeled winter period F_s accounted for between 23% and 29% of annual F_s across the 6-year period [i.e. a range of 6% of annual F_s or 49 g C m⁻² yr⁻¹, which could account for only 11% of the range of interannual variability of F_s (427 g C m⁻² yr⁻¹]. In addition, in 2007, a four-chamber automated Li-8100 system was deployed at the site and between mid-November and the following April recorded a mean F_s of 1.1 μmol m⁻² s⁻¹; this value is consistent with modeled F_s during winter (e.g. Fig. 3) and, therefore, we consider modeled values of F_s during winter to be robust and not a substantial source of interannual variability in F_s .

Across the 6-year period, 2003 was the warmest year and 2006 the wettest; however, annual F_s in both years was close to the 6-year average (i.e. gray bars close to zero in Fig. 2). The years with the lowest and highest annual F_s were 2001 and 2004, respectively, and differed by 427 g C m⁻² yr⁻¹. Early spring snow depth, an indicator of previous winter snowfall, was almost zero in 2001, 2003 and 2005 and approximately 0.44 m in 2002, 2004 and 2006 (Fig. 2). Such patterns appear unrelated to interannual variability in F_s or surface soil moisture. A winter with more than average snow depth may not necessarily equate to a wetter winter because precipitation may arrive as rainfall before or after freezing conditions dominate, and runoff is greater during rain-on-snow events. Over the 6-year period, there was some evidence of increasing average annual water content in the surface layer of the soil; 2001 through 2003 exhibited below-average soil moisture contents whereas 2004 and 2006 exhibited above-average soil moisture contents. Interannual variability in F_s closely followed patterns in tree basal increment ($r^2 = 0.70$, $P = 0.04$), a surrogate for above-ground net primary productivity (ANPP), with almost exclusively higher-than-average F_s in years with higher-than-average ANPP. Previously, we found a strong correlation between annual soil respiration and ANPP in ponderosa pine ecosystems across a range of forest ages and after wildfire (Irvine *et al.*, 2007). The data suggest that interannual variability in F_s shows greater linear correspondence to variables related to photosynthesis than to soil temperature or moisture regimes.

Monthly anomalies in F_s (i.e. black bars in Fig. 2) do not show any consistent correlations with anomalies in soil temperature or moisture. Although the underlying response of F_s to soil temperature is positive and F_s is reduced as soil moisture declines, the interactive nonlinear responses of F_s to both these variables masks the nature of the response of F_s to either variable independently when presenting data as monthly anomalies.

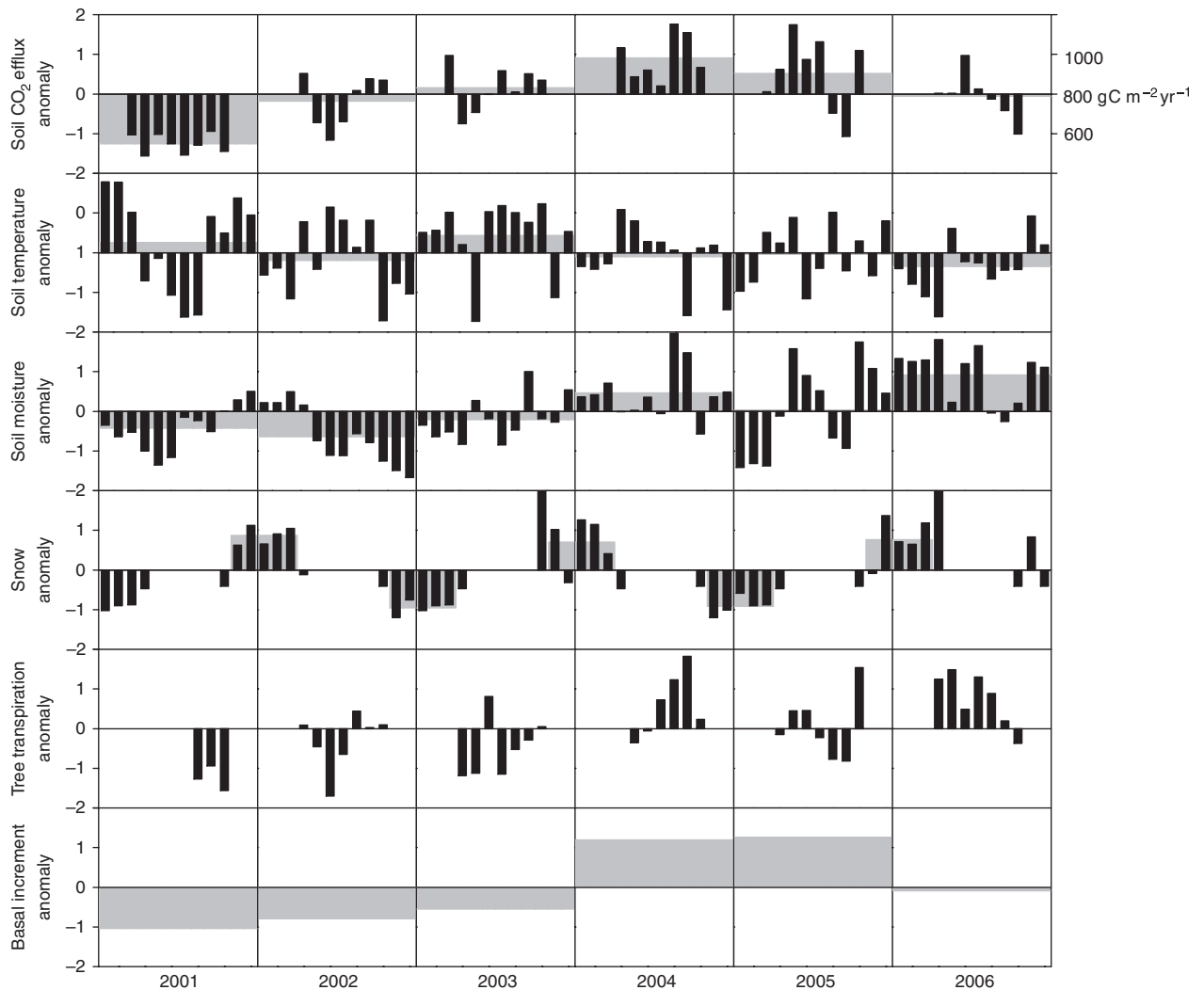


Fig. 2 Interannual and monthly patterns of measured soil CO₂ efflux, soil temperature at 16 cm depth, soil moisture content at 10 cm depth, snow depth, tree transpiration and tree basal area increment. Values are expressed in standard deviations from the 6-year mean on a monthly (black bars) as well as on an annual (gray bars) basis. Annual deviation for snow depth is based on November through March snow season. No annual deviation for tree transpiration is shown as only summer and fall transpiration was measured during 2001. A zero anomaly represents the 6-year mean.

Modeling interannual variability in F_s

With the aim of modeling F_s at the daily scale and capturing interannual variability in F_s , we found that the most generally applicable and parsimonious use of Eqn (1) involved a constant temperature and soil water sensitivity (k_1 through k_3 as constants, see modeling F_s in 'Materials and methods') but a variable R_b that was optimized each year (Table 1). The optimized R_b values showed a strong positive correlation with values of annual tree BAI, $R_b = 0.33 + 0.51 \times \text{BAI}$ ($r^2 = 0.64$, Table 1) with a significant slope ($P = 0.06$) but the intercept was not significantly different from zero ($P = 0.28$). We found no significant correlation between these R_b

values and annual litterfall, even when the previous year's litterfall was used to approximate litter availability for current decomposition. However, the highest annual F_s occurred in the year after the highest litterfall value (Table 1). When combining F_s data from a wide range of sites >40% of maximum seasonal F_s could be accounted for using previous year litterfall (Hibbard *et al.*, 2005). On the basis that the relationship between R_b and BAI had a significant slope but insignificant intercept, we redefined R_b in Eqn (1) as a fraction of annual BAI, which when optimized (with k_1 through k_3 as constants as defined previously) resulted in $R_b = 0.73 \times \text{BAI}$. Annual tree BAI is a good linear proxy for annual change in bolewood volume

and ANPP at this site. If below-ground carbon allocation does not change significantly over the 6 years of the study, the years with high ANPP would also likely show higher-than-average total below-ground carbon allocation. BAI was directly measured in this study; however, many allometric equations for bolewood volume are based on DBH^2 , which could be considered a substitute for BAI in Eqn (1).

To illustrate the suitability of this simplified parameterization of Eqn (1) (i.e. only R_b allowed to vary between years, k_1 through k_3 as constants), we compared the fit with that from the best modeled estimate [i.e. all parameters in Eqn (1) allowed to vary by year; see Fig. 3 for a typical example]. This comparison is given on both a goodness of fit with measured values (Table 1) and also absolute predicted F_s basis (Fig. 4, compare black and gray bars). To make the comparison robust, we excluded the winter period as no measured data were available to tightly constrain modeled esti-

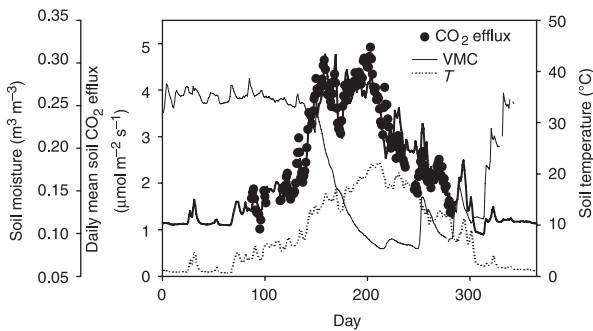


Fig. 3 Example of seasonality of measured daily mean soil CO₂ efflux during 2003 in relation to soil temperature at 16 cm depth (dotted line), soil moisture at 10 cm depth (fine solid line). Overlaid is modeled soil CO₂ efflux (heavy solid line) estimated using Eqn (1) fitted to 2003 data allowing all parameters to vary to generate ‘best’ estimate of annual efflux ($r^2 = 0.86$, Table 1).

mates for that period. In essence, we wish to ascertain if the simplified parameterization of Eqn (1) (i.e. only R_b allowed to vary annually with BAI) can adequately capture interannual variability.

The best modeled estimate of F_s accounted for an average of 85% of the measured values over the 6-year period, compared with 76% using simplified parameterization (Table 1; Fig. 4, compare black and gray bars). Thus, only ~9% more of the variability in F_s could be described by allowing all four parameters in Eqn (1) to vary by year compared with using a fixed sensitivity of F_s to soil temperature and soil moisture, and R_b as a constant fraction of BAI. The simplified model predicted seasonal total F_s to be on average within 13 g C or 3% of the best modeled seasonal F_s (Fig. 4, compare black and gray bars). The interannual patterns in F_s showed a much larger range than the deviations between the best modeled estimates of F_s and the simplified model estimates of F_s such that the interannual variability in F_s was largely captured by the simplified model.

To assess the sensitivity of modeled seasonal total F_s to BAI, we substitute the mean annual BAI over the 6-year period into the simplified model (Fig. 4, white bars). The percentage change in predicted seasonal F_s (Fig. 4, compare gray and white bars, values above white bars are percentage change) showed a range from -15% in 2004 to +15% in 2001; thus, measured changes in BAI over the 6-year period resulted in up to 30% change in modeled seasonal total F_s . Similarly, to assess the sensitivity of F_s to changes in climate, we substitute the mean daily soil temperature and moisture values from the 6-year record into the simplified model (Fig. 4, diagonal hashed bars). The percentage change in predicted seasonal F_s using year-specific R_b – but the average climate – showed a range from -10% in 2004 to +19% in 2001 (Fig. 4, values above diagonal hashed bars); thus the natural variability of climate across the

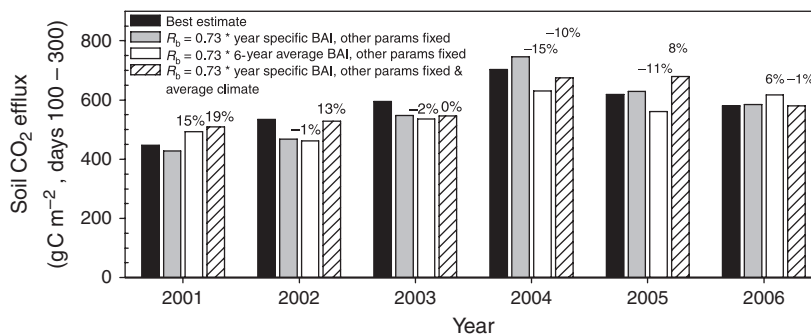


Fig. 4 Comparison of the simplified parameterization (gray bars) of Eqn (1) to estimate seasonal total soil CO₂ efflux with the best estimate (black bars) of seasonal total soil CO₂ efflux. The sensitivity of the simplified model to the interannual variability in tree basal area increment across the 6 years (white bars and percentage change compared with simplified) and the interannual variability in soil climate across the 6 years (diagonal hashed bars and percentage change compared with simplified) is also illustrated (see ‘Modeling interannual variability in F_s ’).

6-year period resulted in modeled seasonal F_s varying by up to 29%. Therefore, both the interannual variability in BAI and the interannual variability in soil climate appear almost equally to account for interannual variability in F_s . Arguably, this approach is simplistic as years with soil climatic conditions that favor high rates of F_s will also likely be the years that favor higher-than-average BAI (i.e. R_b is not independent of the combined influence of soil temperature and moisture on F_s). Wet and warm conditions favor both increased F_s and tree growth. Care needs to be taken interpreting data based on average annual climatic conditions; 2005 had average annual temperature and moisture (Fig. 2) but the substitution of the 6-year daily average climate into the simplified model resulted in an 8% increase in F_s , and the substitution of 6-year average BAI resulted in an 11% decline in F_s , suggesting the year with conditions that favored the highest BAI did not have soil climatic conditions that favored the highest F_s . Average annual statistics mask the relative importance of temperature and moisture at different points during the season. A more detailed analysis of the sensitivity of seasonal total F_s to changes in climate over the 6 years indicated that seasonal total F_s was twice as sensitive to soil moisture variability during the summer months compared with temperature variability during the same period and almost insensitive to the natural range of interannual variability in spring temperatures.

It is clear from the previous discussion that there are limitations on usefulness of empirical relations of F_s to soil climate and ANPP to infer the underlying mechanisms. However, a simplified parameterization of Eqn (1) that only allows R_b to vary with BAI and sets all other parameters to constants can adequately represent more than three-quarters of the variability in F_s . To make further progress, it is necessary to break F_s into smaller components.

Separation of F_s into autotrophic and heterotrophic components

Here, we consider soil R_r to include any CO_2 release directly from roots and from root exudates metabolized by rhizosphere organisms. We consider soil R_h to originate from other micro-organisms including fungi in both the bulk soil and litter layer that do not depend directly on root compounds. Thus, F_s in the root exclusion treatment is assumed to be R_h . F_s from the control treatment is a combination of R_r and R_h .

Data used in this analysis were only included if at least four out of six chambers in the control treatment and at least three out of four chambers in the root exclusion treatment were functioning each day. Before the root exclusion plots were trenched on July 22, 2004

(day 204, vertical line; Fig. 5), F_s in both treatments differed only due to inherent spatial variation of F_s across the forest floor. Pretrenched root exclusion F_s averaged 78% of control F_s , and this value was used to correct data subsequent to trenching for values shown in the lower two panels in Fig. 5. We also estimated R_h in the root exclusion plots and it was overestimated by 15% due to the artificial addition of severed roots; this figure was based on measurements of root mass and decomposition rates, and is close to the average value of 12% reported from across a number of root exclusion studies (Subke *et al.*, 2006). We found 540 g C m^{-2} in live fine roots (up to 2 mm diameter) to 1 m soil depth of which approximately 26% were estimated to decompose within the first 3 months (Chen *et al.*, 2002) followed by a slower decay rate of 12% a year for ponderosa pine (Law *et al.*, 2001). Because most information from the root exclusion study presented here was collected during 2005, at least 7 months after roots were severed, we applied the decomposition rate of 12% a year to correct data throughout after reducing the fine root pool size by 26%. The decomposition of large roots was also estimated in a similar manner using decay constants reported by Chen *et al.* (2001). Using this approach, we estimate approximately 6% of daily F_s in the root exclusion plots originated from decomposition of fine roots killed during trenching and an additional 7% from decomposition of larger roots. The data shown in Fig. 5, lower two panels, have been corrected for this overestimation of R_h .

There were no discernable differences in the magnitude and seasonality in soil temperature in the two treatments (Fig. 5, second panel down). Soil water content showed typical patterns of winter and early spring recharge followed by summer depletion. Soil water content in both treatments tracked each other in 2004 until several large rain events occurred in mid- to late August 2004 (day 229–238, 42 mm total). In response, both treatments showed an increase in soil moisture but the subsequent rate of soil water depletion was greater in the control treatment where roots deplete soil moisture. More detailed measurements of soil water content by depth also suggested that these heavy rainfall events were only detected in the top 30 cm of soil in the root exclusion treatment but detected to approximately twice this depth in the control treatment suggesting hydraulic redistribution from the surface layer to layers deeper in the profile by roots (data not shown). The response of R_h to these rain events, relative to prerin values, was more than twice as large as the response of R_r . During the unusually wet August and September, R_r was on average 38% of total F_s and remained fairly stable until declining sharply in early October.

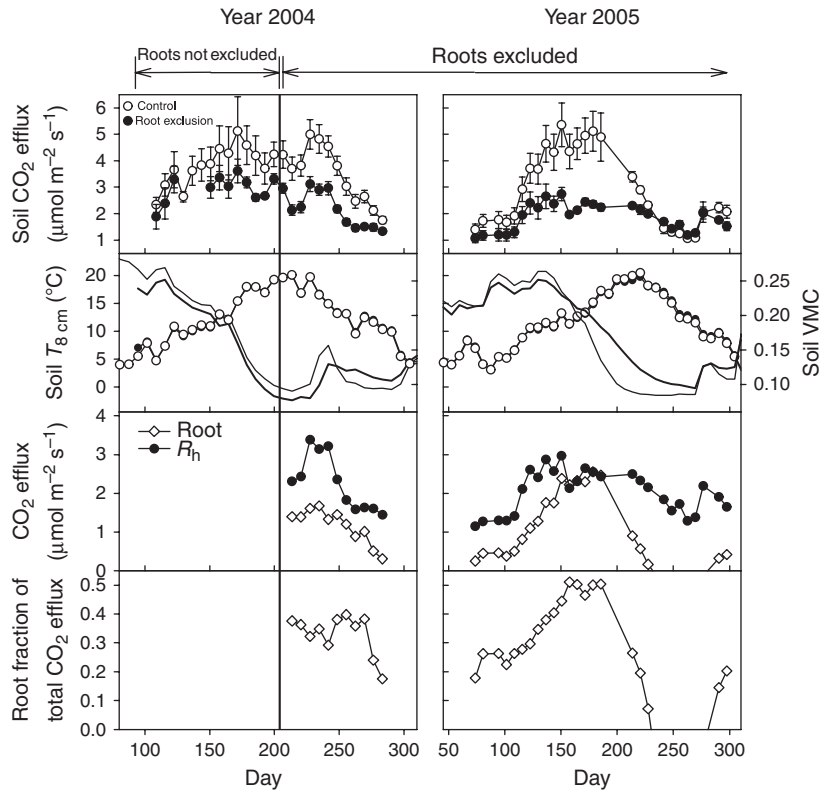


Fig. 5 Seasonality in root (R_r) and soil heterotrophic (R_h) respiration during late 2004 and 2005, and associated soil climatic conditions. The combination of R_r and R_h is measured in the control treatment, whereas in the root exclusion treatment, all the data following trenching (Day 204, 2004, vertical line) are a result of R_h . After accounting for the offset between treatments before root exclusion, and the artifact of higher R_h in the exclusion treatment (due to added severed roots), the ratio's among treatments allow calculation of R_r and R_h (lower two sets of panels). Mean weekly values of all variables are presented, error bars \pm SE. Second panel down: soil temperature (○: control, ●: root exclusion) and soil moisture content (fine line control, heavy line root exclusion).

In 2005, a strong seasonality in both R_r and R_h was observed (Fig. 5, lower two panels) with both R_r and R_h increasing during spring. R_h remained stable, albeit with some variability, between mid-May and mid-August before declining in early October. R_h recovered briefly with autumn rainfall. The stability in R_h during the summer months appeared to be due to a constraint by soil moisture availability from about late June such that as soil temperature increased, a concurrent decline in soil moisture was observed. The combined behavior of R_r and R_h during the 2005 season resulted in the fraction attributed to R_r increasing steady from 18% in mid-March to 50% in early June. The fraction R_r remained at 50% until early July before dropping rapidly to 10% of total F_s by mid-August. Because measurements of R_r and R_h were not available during the winter months, we assume the fraction of F_s attributed to R_r during this period was 22% based on the value measured in March 2005, and also assume that during September, R_r negligibly contributed to F_s ; then annually, R_r accounted for 26% of F_s . We note that this is

not the average monthly R_r fraction of F_s across 12 months but the annual sum of R_r as a fraction of total F_s . This fraction was lower than expected due to an artifact of trenching such that in July 2005, the rate of decline of soil moisture in the trenched plots was reduced compared with the control plots which likely resulted in an overestimation of the fraction of R_h during late summer 2005. Limited data were available during this period in part due to gas analyzer failure (gap ~day 189–213) such that we were unable to develop a robust empirical relationship for R_h -based soil moisture and temperature that could be used to correct for this artifact. If we assume that the fraction R_h during August and September 2005 was similar to the values measured during June, this would result in R_r accounting for 38% of F_s on an annual basis.

The unusually heavy rainfall in late summer 2004 mitigated drought stress and tree transpiration, a proxy for carbon assimilation, showed much higher rates in August and September 2004 compared with the same months in 2005 (Fig. 6). Seasonal changes in R_r and tree

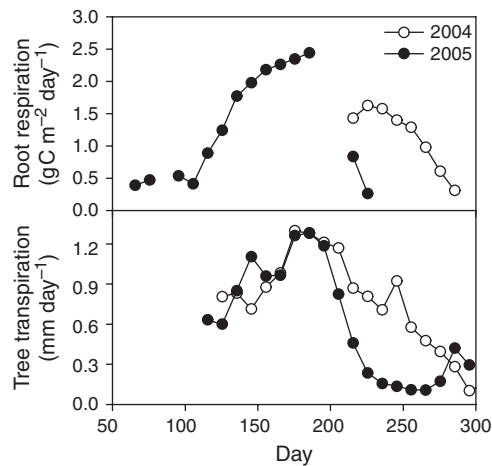


Fig. 6 Ten-day average root respiration and tree transpiration during 2004 and 2005.

transpiration were very similar and 10-day averages were strongly linearly correlated ($r^2 = 0.90$, $P < 0.01$). Ten-day average GEP estimated from eddy-flux data showed a strong linear relationship with R_r ($r^2 = 0.83$, $P < 0.01$). R_r increased by $0.43 \text{ gC m}^{-2} \text{ day}^{-1}$ for every $1 \text{ gC m}^{-2} \text{ day}^{-1}$ increase in GEP (Fig. 7). We note that the underestimation of R_h in late summer 2005 would only influence 3 of the 22 data points presented in Fig. 7 and thus not substantially alter the presented relationships.

Techniques available to separate R_r and R_h in the field are limited (for a summary of approaches see Subke *et al.*, 2006) and each suffers from various limitations and resulting artifacts. One potential issue with the trenching approach is that rhizosphere priming is eliminated, which may result in changed rates of decomposition of older organic material. However, there is no consensus of the degree of importance of this process and whether it will result in higher or lower rates of R_h (Kuzyakov, 2006).

Synthesis

In this seasonally water-limited ecosystem, we observed strong seasonal patterns in the underlying processes contributing to F_s as has been observed in a wide range of forest types in both temperate (Epron *et al.*, 2001; Wang & Yang, 2006) and boreal (Hogberg *et al.*, 2001; Bond-Lamberty *et al.*, 2004; Gaumont-Guay *et al.*, 2008) ecosystems. Combined, these studies indicate that the increase in the fraction of R_r during the peak growing season is directly linked to seasonal patterns of GEP, which is influenced by edaphic and climatic conditions (Ryan & Law, 2005). The exact connection between GEP and R_r remains an active area of research; in a boreal black spruce stand, a lag of several weeks between seasonal maximum GEP and R_r was observed (Gaumont-Guay *et al.*, 2008). But in

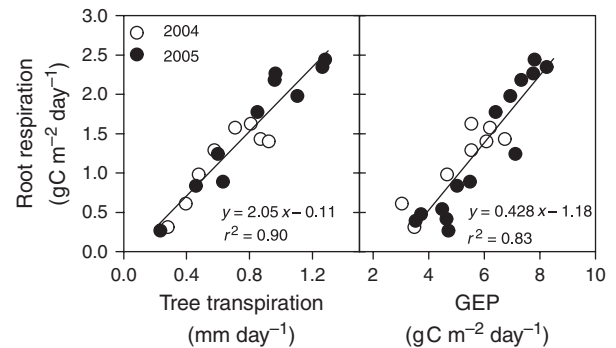


Fig. 7 Root respiration (R_r) in relation to tree transpiration (sap flux measurements) and gross ecosystem productivity (eddy correlation) during late 2004 and 2005. Values shown are 10-day average values for all variables.

a Scots pine stand, a more immediate reduction in R_r was observed following stem girdling (Hogberg *et al.*, 2001), and subsequent research using pulse labeling confirmed that recent photosynthates were detected in the roots after only a few days (Hogberg *et al.*, 2008). In the current study, we found canopy gas exchange and R_r varied in concert throughout the growing season. Measurements were made in both unusually wet and more typical water limited summer conditions and striking correlations were observed among R_r , GEP and tree transpiration. In a much younger pine stand, we also observed that by independently manipulating the rate of transpiration and photosynthesis, and measuring the concurrent change in R_r , a strong linear dependency was observed between these processes on the daily scale (Irvine *et al.*, 2005). While such observations are not a demonstration of cause and effect, they strongly suggest that seasonal patterns in R_r are driven directly by changes in GEP.

The large interannual variability in F_s observed in this study is consistent with observations in both more xeric (Asensio *et al.*, 2007) and more mesic forest ecosystems (Savage & Davidson, 2001). Although a growing number of publications relate F_s to site productivity or surrogates such as LAI (e.g. Reichstein *et al.*, 2003), such relationships are usually generated from data collected from across wide geographical gradients. Few publications have attempted to relate interannual variability of F_s in forested ecosystems to both climatic variability and above-ground plant productivity, although Epron *et al.* (2004) attributed interannual variability in F_s to the changing basal rate of F_s rather than changing temperature sensitivity. The time course, Epron *et al.* (2004) present of the R_b of F_s appears consistent with the annual increase in tree biomass. More long-term datasets of F_s and above-ground measures of plant productivity are needed to determine the strength of the connection

between GEP and F_s . In a grassland ecosystem, Dornbush & Raich (2006) concluded that temporal patterns in F_s were more related to changes in soil temperature than ANPP. Such observations highlight the need to determine the nature of above- to below-ground carbon coupling in different plant functional types.

Considering the highly dynamic nature of the underlying components of F_s , empirical efforts at modeling the seasonality in F_s by changing the basal rate of respiration or the temperature sensitivity of F_s will not likely help resolve the underlying processes, especially in ecosystems where factors other than temperature control F_s . However, on an interannual time scale, we observed that annual ANPP proved to be strongly correlated with the annual basal rate of F_s . When this R_b is modulated with fixed sensitivity to temperature and soil water availability on a daily scale, seasonal patterns in F_s were estimated well across the 6 years of observations.

With current concerns about global climate change and the role terrestrial ecosystems may play in sequestering carbon, it is important to quantify and understand interannual variability in net carbon uptake. Roughly 80% of carbon taken up by photosynthesis in forests is returned to the atmosphere via respiration, much of which is from the soil (Law *et al.*, 2001). Ongoing development of various models to better capture interannual variability in NEE indicates the need for long-term continuous observations of soil respiration and its components in addition to NEE to diagnose model representation of ecosystem processes.

Acknowledgements

This research was supported by the U.S. Department of Energy, Terrestrial Carbon Program (DOE Grant no. DE-FG02-06ER64318), for the AmeriFlux project on the effects of disturbance and climate on carbon storage and the exchanges of CO_2 , water vapor and energy exchange of evergreen coniferous forests in the Pacific Northwest: integration of eddy-flux, plant and soil measurements at a cluster of supersites. We gratefully acknowledge Amy Burke and Cody Pepper for field assistance and Heath Powers for maintaining equipment and processing data.

References

Anthoni PM, Unsworth MH, Law BE, Irvine J, Baldocchi D, Van Tuyl S, Moore D (2002) Seasonal differences in carbon and water vapor exchange in young and old-growth ponderosa pine ecosystems. *Agricultural and Forest Meteorology*, **111**, 203–222.

Asensio D, Penuelas J, Llusia J, Ogaya R, Filella I (2007) Interannual and interseasonal soil CO_2 efflux and VOC exchange rates in a Mediterranean holm oak forest in response to environmental drought. *Soil Biology and Biogeochemistry*, **39**, 2471–2484.

Bond-Lamberty B, Wang C, Gower ST (2004) Contribution of root respiration to soil surface CO_2 flux in a boreal black spruce chronosequence. *Tree Physiology*, **24**, 1387–1395.

Chen H, Harmon ME, Griffiths RP (2001) Decomposition and nitrogen release from decomposing woody roots in coniferous forests of the Pacific Northwest: a chronosequence approach. *Canadian Journal of Forest Research*, **31**, 246–260.

Chen H, Harmon ME, Sexton J, Fasth B (2002) Fine root decomposition and N dynamics in coniferous forests of the Pacific Northwest, USA. *Canadian Journal of Forest Research*, **32**, 320–331.

Curiel Yuste J, Janssens IA, Carrara A, Ceulemans R (2004) Annual Q_{10} of soil respiration reflects plant physiological patterns as well as temperature sensitivity. *Global Change Biology*, **10**, 161–169.

Davidson EA, Janssens IA (2006) Temperature sensitivity of soil carbon decomposition and feedbacks to climate change. *Nature*, **440**, 165–173.

Davidson EA, Janssens IA, Luo Y (2005) On the variability of respiration in terrestrial ecosystems: moving beyond Q_{10} . *Global Change Biology*, **11**, 1–11.

Dornbush ME, Raich JW (2006) Soil temperature, not aboveground plant productivity, best predicts intra-annual variations of soil respiration in central Iowa grasslands. *Ecosystems*, **9**, 909–920.

Epron D, Le Dantec V, Dufrene E, Granier A (2001) Seasonal dynamics of soil carbon dioxide efflux and simulated rhizosphere respiration in a beech forest. *Tree Physiology*, **21**, 145–152.

Epron D, Ngao J, Granier A (2004) Interannual variation of soil respiration in a beech forest ecosystem over a six-year study. *Annals of Forest Science*, **61**, 499–505.

Falge E, Baldocchi D, Olson R *et al.* (2001) Gap filling strategies for defensible annual sums of net ecosystem exchange. *Agricultural and Forest Meteorology*, **107**, 43–69.

Gaumont-Guay D, Black TA, Barr A, Jassal RS, Nesic Z (2008) Biophysical controls on rhizospheric and heterotrophic components of soil respiration in a boreal black spruce stand. *Tree Physiology*, **28**, 161–171.

Goulden ML, Crill PM (1997) Automated measurements of CO_2 exchange at the moss surface of a black spruce forest. *Tree Physiology*, **17**, 537–542.

Goulden ML, Munger JW, Fan SM, Daube BC, Wofsy SC (1996) Measurements of carbon sequestration by long-term eddy covariance: methods and a critical evaluation of accuracy. *Global Change Biology*, **2**, 169–182.

Gu L, Falge EM, Boden T *et al.* (2005) Objective threshold determination for nighttime eddy flux filtering. *Agricultural and Forest Meteorology*, **128**, 179–197.

Hanson PJ, Edwards NT, Garten CT, Andrews JA (2000) Separating root and soil microbial contributions to soil respiration: a review of methods and observations. *Biogeochemistry*, **48**, 115–146.

Hibbard KA, Law BE, Reichstein M, Sulzman J (2005) An analysis of soil respiration across northern hemisphere temperate ecosystems. *Biogeochemistry*, **73**, 29–70.

Hogberg P, Hogberg MN, Gottlicher SG *et al.* (2008) High temporal resolution tracing of photosynthate carbon from the tree canopy to forest soil microorganisms. *New Phytologist*, **177**, 220–228.

- Hogberg P, Nordgren A, Buchmann N *et al.* (2001) Large-scale forest girdling shows that current photosynthesis drives soil respiration. *Nature*, **411**, 789–792.
- Hogberg P, Read DJ (2006) Towards a more plant physiological perspective on soil ecology. *Trends in Ecology and Evolution*, **21**, 548–554.
- Irvine J, Law BE (2002) Contrasting soil respiration in young and old-growth ponderosa pine forests. *Global Change Biology*, **8**, 1183–1194.
- Irvine J, Law BE, Hibbard KA (2007) Postfire carbon pools and fluxes in semiarid ponderosa pine in Central Oregon. *Global Change Biology*, **13**, 1748–1760.
- Irvine J, Law BE, Kurpius MR (2005) Coupling of canopy gas exchange with root and rhizosphere respiration in a semi-arid forest. *Biogeochemistry*, **73**, 271–282.
- Irvine J, Law BE, Kurpius MR, Anthoni PM, Moore D, Schwarz PA (2004) Age-related changes in ecosystem structure and function and effects on water and carbon exchange in ponderosa pine. *Tree Physiology*, **24**, 753–763.
- Janssens IA, Lankreijer H, Matteucci G *et al.* (2001) Productivity overshadows temperature in determining soil and ecosystem respiration across European forests. *Global Change Biology*, **7**, 269–278.
- Kuzyakov Y (2006) Sources of CO₂ efflux from the soil and review of partitioning methods. *Soil Biology and Biogeochemistry*, **38**, 425–448.
- Law BE, Baldocchi DD, Anthoni PM (1999) Below-canopy and soil CO₂ fluxes in a ponderosa pine forest. *Agricultural and Forest Meteorology*, **94**, 13–30.
- Law BE, Thornton P, Irvine J, Anthoni PM, Van Tuyl S (2001) Carbon storage and fluxes in ponderosa pine forests at different developmental stages. *Global Change Biology*, **7**, 755–777.
- Luo Y, Zhou X (eds) (2007) Modeling synthesis and analysis. In: *Soil Respiration and the Environment*, pp. 215–246. Elsevier, Amsterdam.
- Raich JW, Potter CS, Bhagawati D (2002) Interannual variability in global soil respiration, 1980–94. *Global Change Biology*, **8**, 800–812.
- Reichstein M, Falge E, Baldocchi D *et al.* (2005) On the separation of net ecosystem exchange into assimilation and ecosystem respiration: review and improved algorithm. *Global Change Biology*, **11**, 1424–1439.
- Reichstein M, Rey A, Freibauer A *et al.* (2003) Modeling temporal and large-scale spatial variability of soil respiration from soil water availability, temperature and vegetation productivity indices. *Global Biogeochemical Cycles*, **17**, 1104, doi: 10.1029/2003GB002035.
- Ryan MG, Law BE (2005) Interpreting, measuring and modeling soil respiration. *Biogeochemistry*, **73**, 3–27.
- Sampson DA, Janssens IA, Yuste JC, Ceulemans R (2007) Basal rates of soil respiration are correlated with photosynthesis in a mixed temperate forest. *Global Change Biology*, **13**, 2008–2017.
- Savage KE, Davidson EA (2001) Interannual variation of soil respiration in two New England forests. *Global Biogeochemical Cycles*, **15**, 337–350.
- Stoy PC, Palmroth S, Oishi AC *et al.* (2007) Are ecosystem carbon inputs and outputs coupled at short time scales? A case study from adjacent pine and hardwood forests using impulse-response analysis. *Plant Cell and Environment*, **30**, 700–710.
- Subke JA, Inghima I, Cotrufo MF (2006) Trends and methodological impacts in soil CO₂ efflux partitioning: a metaanalytical review. *Global Change Biology*, **12**, 1–23.
- Wang C, Yang J (2006) Rhizosphere and heterotrophic components of soil respiration in six Chinese temperate forests. *Global Change Biology*, **13**, 123–131.